Preprints of the 21st IFAC World Congress (Virtual)
Berlin, Germany, July 12-17, 2020

Model-Based End of Discharge Temperature Prediction for Lithium-Ion Batteries

**Mona Faraji-Niri*, Truong M.N. Bui*,
Tung Fai Yu**, James Marco ***

** Energy innovation Centre, Warwick Manufacturing Group, University of Warwick, Coventry, CV4 7AL, United Kingdom, (Emails: Mona.Faraji-Niri@warwick.ac.uk, T.Bui.2@warwick.ac.uk, and James.Marco@warwick.ac.uk)*
*** Advanced Battery Engineering, Jaguar Land Rover Ltd, Coventry, CV3 4LF, United Kingdom tyu5@jaguarlandrover.com*

Abstract: Battery fast charging is one of the key techniques that affects the public acceptability and commercialization of electric vehicles. Temperature is the critical barrier for fast charging as at low temperatures an increased risk of lithium plating and at high temperatures safety concerns limits the charging rate. To facilitate a fast charging mechanism, preconditioning the battery and maintaining its temperature is vital. Battery temperature prediction before a fast charging event can help reducing the energy consumption for battery preconditioning. In this paper, we propose a method for battery end of discharge temperature prediction for fast charging purposes. Firstly, a Gaussian mixture data clustering is performed on battery load data characterisation, subsequently a Markov model is trained for load prediction, and finally a battery lumped parameter equivalent circuit and thermal model is developed and employed for end of discharge time and ultimately end of discharge temperature prediction. Cylindrical lithium-ion battery is selected to prove the concept and both simulations and experiments show the capabilities of the proposed method for temperature prediction of batteries under load profiles obtained from real-world drive cycles of electric vehicles.

Keywords: Gaussian mixture data clustering, Markov model, transient load, Lithium-ion battery, Temperature prediction, Fast Charging.

1. INTRODUCTION

Recent years have witnessed considerable development in the lithium-ion based electric vehicles (EVs). Compared to the combustion engine vehicles that can be refuelled very quickly, charging the battery pack of electric vehicles may require several minutes and even hours depending on the vehicle and ambient conditions. Longer charging time of EVs is one of the items causing range anxiety, the fear of not reaching the destination due to the lack of charge, as the vehicle gets out of service during the charging. Having access to fast chargeable EVs and their relevant infrastructures may ease the range anxiety. Studies show a 25% increase in the annual mileage travelled by EVs in areas with fast charging stations (Lutsey, et al., 2015). Therefore, reduced charging time and guaranteed safe procedure is one of the highly significant features in modern EVs. Even though charging process can be accelerated by high currents but it has a negative effect on the battery energy efficiency and cause power and capacity fade as well as impedance rise. That's why fast charging is considered a multiscale problem and atomic, micro, cell, pack and system level studies are required to address it (Tomaszewska, et al., 2019).

The rate of the energy fed into the lithium-ion battery is critically dependent to the temperature. When the temperature is low, charging events may increase the risk of lithium plating (Cabañero, et al., 2019), (Wandt, et al., 2018). The most considerable outcome of lithium plating is the capacity loss, the possibility of internal short circuit, safety issues, and reduced durability and reliability of the battery pack. On the other hand, when the temperature is high, feeding the external energy into the battery is faster but this may accelerate the internal side reactions, change thermal runaway characteristics and increase the risk of fire or even an explosion.

Generally charging speed and efficiency reduces at lower temperatures (Yang & Wang , 2018). For example, charging Nissan LEAF with a 40-62 kWh battery pack and a 50kW charger can take from 30 to 90 minutes depending on the temperature (Tech. rep., 2014) and the fast charging is only applicable up to 80% of state of charge (SoC) as at higher SoCs the current slightly decreases to avoid hitting the upper voltage limits of the battery which in turn leads to longer charge times (Mussa, et al., 2017). The efficiency of fast charging can reduce from 93% to 39% when the temperature goes from 25 C to -25 for a 50 kW charger (Trentadue, et al., 2018). Accordingly, it is truly challenging to make the lithium-ion battery charging independent of the temperature (Yang, et al., 2018). While the battery charging protocols are mostly defined by the manufacturers, the battery discharge and its temperature is affected by the driver behaviour and the ambient conditions. For fast charging it is important to keep the battery temperature above a limit to avoid lithium plating and below a maximum to keep it safe. Generally in EVs, first the battery temperature is transformed to an optimal temperature and then the charging event starts. This is performed by the battery heating device and usually by applying an external current to the battery (Yang, et al., 2018).

In fast charging rapid internal heating of the battery is essential to keep the charging time between 10 to 15 minutes. However

rapid heating may lead to a non-uniform heat distribution in the cell with local overheated patches near the cell surface (Yang, et al., 2017). This limits the heating rate to 1°C per minute (Ji & Wang, 2013) which means heating up the battery from 0 to 20 °C will take 20 minutes which added to the 15 minutes of charging itself, takes the whole process out of the fast charging category.

Considering the abovementioned challenges, thermal management strategies for preheating the battery have a crucial impact on fast charging process efficiency. Preheating the battery via external currents requires energy consumption and also accelerates the battery ageing. Specifically, if the battery temperature can be predicted before a fast charging event then the thermal management system can adjust the battery temperature via a suitable heating rate to reach the optimal temperature. In fact instead of cooling the battery continuously and then heating it up immediately before a fast charge, knowing the end of discharge temperature, the cooling mechanism can be controlled such that the battery temperature increase naturally as it is cycled until a fast charge start. In this case the battery will be already warm and will require less energy for reheating. Motivated by this requirement, this paper focuses on the end of discharge (EoD) temperature prediction for thermal management purposes. To the best of the authors' knowledge, this problem has not been addressed so far in the field of battery studies.

Here, first a load prediction algorithm is designed based on the load data clustering and stochastic modelling to obtain the most possible future trend for the battery. The algorithms is based on Markov decision processes which have been addressed for many applications of load prediction in vehicular technology (Jiang & Fei, 2015; Zou, et al., 2016; Faraji Niri, et al., 2020; Faraji Niri, et al., 2019). Markov process have strong prediction capabilities for highly transient data subject to uncertainty. The proposed algorithm utilises the historical data of the battery usage and adds levels of uncertainty to it to cover future stochastic conditions. The predicted load is applied to a battery electrical-thermal model to get the end of discharge time and the end of discharge temperature. To further show the advantages of the temperature prediction algorithm, the results are compared with the moving average load prediction method as well. The algorithm is verified via simulations and experiments under two loading scenarios coming from real drive cycles of electric vehicles at different temperatures. The organization of paper is as follows: in Section 2 the battery electrical-thermal model is developed. Load prediction algorithm via Gaussian mixture model and Markov process is given in Section 3. Section 4 gives the simulation and experimental results as well as comparisons. Finally, Section 5 concludes the paper.

2. BATTERY ELECTRICAL-THERMAL MODEL DEVELOPMENT

While the present battery current, voltage and temperature are measurable via sensors, an accurate battery model is required to obtain the future values of these signals. Battery electrical model helps to predict the voltage and get its end of discharge time and a battery thermal model helps to forecast the battery temperature. Equivalent circuit model (ECM) is widely used in on-board state estimation applications due to its affordable computational complexity (Hu , et al., 2012). Based on (Wu, et al., 2010), (Zhang & Peng, 2017) it is concluded that a second order ECM, Fig.1, is a suitable candidate for battery management system (BMS) applications. The model contains an internal resistance of R_0, two polarization resistances of R_1, R_2 and two polarization capacitances of C_1, C_2.

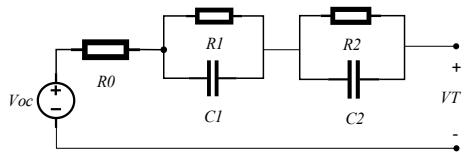

Fig.1. Schematic of second order ECM

The output voltage of the battery is described via the following equations, where v_{p1} and v_{p2} are the RC branch polarization voltage, V_{oc} is the open circuit voltage, I is the battery load current and T_1, T_2 are model time constants.

$$\begin{aligned} \dot{v}_{p1} &= -\frac{v_{p_1}}{R_1C_1} + \frac{I}{C_1}, \\ T_1 &= R_1C_1, \\ \dot{v}_{p2} &= -\frac{v_{p2}}{R_2C_2} + \frac{I}{C_2}, \\ T_2 &= R_2C_2 \\ V_T &= V_{OC} - \sum_{i=1}^{2} v_{pi} - R_0 I \end{aligned} \tag{1}$$

To address the thermal behaviour of the battery in this study the model developed by (Kim, et al., 2013) is employed. The model considers the radially distributed heat in a cylindrical cell with convective heat transfer boundary conditions. Assuming a uniform heat generation, the governing temperature distribution and boundary conditions are given by

$$\begin{aligned} \rho c_p \frac{\partial T}{\partial t} &= \frac{Q}{V_b} + k_t \frac{\partial^2 T}{\partial r^2} + \frac{k_t}{r}\frac{\partial T}{\partial r} \\ \frac{\partial T}{\partial r}|_{r=R} &= -\frac{h}{k_t}(T - T_\infty), \quad \frac{\partial T}{\partial r}|_{r=0} = 0 \end{aligned} \tag{2}$$

where ρ, c_p, k_t and h are volume averaged cell density, specific heat coefficient, thermal conductivity and convection coefficient. R, V_b and T_∞ are the cell radius, bulk volume and the ambient temperature.

To overcome the computational complexity of the partial differential equation (PDE) of (2) a polynomial is used to approximate the PDE solution (Subramanian, et al., 2005). Considering the polynomial approximation along r-direction as well as the volume-averaged temperature, $\bar{T}$ and temperature gradient $\bar{\gamma}$ as,

$$\bar{T} = \frac{2}{R^2}\int_0^R rTdr,\ \ \bar{\gamma} = \frac{2}{R^2}\int_0^R r\frac{\partial T}{\partial r}dr \tag{3}$$

a two state temperature model can be obtained by the following state space form where $\alpha = k_t/\rho c_p$ is thermal diffusivity and Q is the generated heat with V_b as the bulk cell volume.

$$\begin{bmatrix}\dot{\bar{T}}\\ \dot{\bar{\gamma}}\end{bmatrix} = \begin{bmatrix}\frac{-48\alpha h}{R(24k_t+Rh)} & \frac{-15\alpha h}{24k_t+Rh}\\ \frac{-320\alpha h}{R^2(24k_t+Rh)} & \frac{-120\alpha(4k_t+Rh)}{R^2(24k_t+Rh)}\end{bmatrix}\begin{bmatrix}\bar{T}\\ \bar{\gamma}\end{bmatrix} + \begin{bmatrix}\frac{\alpha}{k_tV_b} & \frac{48\alpha h}{R(24k_t+Rh)}\\ 0 & \frac{-320\alpha h}{R^2(24k_t+Rh)}\end{bmatrix}\begin{bmatrix}Q\\ T_\infty\end{bmatrix} \tag{4}$$

$$[T] = \begin{bmatrix}\frac{24k_t}{24k_t+Rh} & \frac{15Rk_t}{48k_t+2Rh}\end{bmatrix}\begin{bmatrix}\bar{T}\\ \bar{\gamma}\end{bmatrix} + \begin{bmatrix}0 & \frac{Rh}{24k_t+Rh}\end{bmatrix}\begin{bmatrix}Q\\ T_\infty\end{bmatrix}$$

The battery heat generation is expressed by (5). It only considers irreversible heat generation mechanisms and assumes a negligible heat generation due to reversible mechanisms, entropy of mixing, phase and heat capacity change (Bernardi, et al., 1985).

$$Q = I(V_{oc} - V_T) \tag{5}$$

3. END OF DISCHARGE TEMPERATURE PREDICTION

In order to find the EoD temperature, the load profile from the present time point t to the EoD time of the battery is required. In real operation conditions the future load profile is uncertain. To deal with the ubiquitous future conditions a load prediction mechanism is required. Here systematic load prediction is performed which utilises the historical data to identify the charge/discharge trend and generate future realizations of load via a stochastic model.

The stochastic load prediction mechanism is formed by a coupled Gaussian mixture and Markov model. The block diagram of the prediction algorithm is given at Fig. 2.

The Markov model in this algorithm is consisted of a finite number of states S_t, in set of $\underline{N}=\{1, \dots, N\}$, the switching between these states follows the probabilities of (6).

$$\Pr\left\{S_{t+T_s} = j \mid S_t = i\right\} = \lambda_{ij}\ \ i, j \in \underline{N} \tag{6}$$

Here, $\lambda_{ij} \geq 0$, $\sum_{j\in\underline{N}}\lambda_{ij} = 1$, is the transition probability (TP) from state i at time t to state j at time $t + T_s$, where T_s is the sampling time.

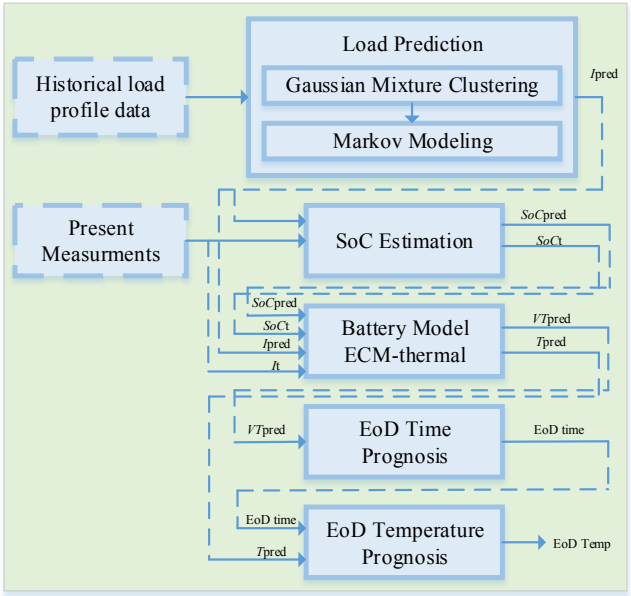

Fig.2. General EoD temperature prediction mechanism

In order to specify the states of the Markov model, a Gaussian mixture clustering algorithm is utilised. Gaussian mixture clustering classifies the load data, x, in finite number of clusters with a normal probability distribution. Via this algorithm the probability density function (PDF) of whole data, $p(x)$, can be modeled by a mixture of Gaussian PDFs as:

$$p(x) = \sum_{m=1}^{M} w_m N(x; \mu_m, \sigma_m) \tag{7}$$

where M is the number of clusters and $N(x;\mu_m,\sigma_m)$ is the Gaussian distribution function of cluster m, with mean μ_m covariance σ_m and weight w_m. Here for simplicity the data of the historical load are quantized into two possibles clusters of S_{low} and S_{high}, which specify the low and high energy cosumption states of the Markov model between t to $t+T_L$, where T_L is the update interval for training the model. For each training interval the TPs are computed via maximum-likelihood (Brooks, et al., 2011) and used for generating the future load state and load value.

Based on the information of future load profiles, the EoD time and EoD temperature are obtained following the definitions of (8), where V_{Tlim} is the cut-off terminal voltage usually specified by the battery manufacturer. It is the voltage threshold below which the battery may face serious safety and performance issues. The Fig. 3 shows the steps of the proposed algorithm.

$$EoD_{Time} = E\{t \mid E\{V_{Tt}\} = V_{T\lim}\}$$
$$EoD_{Temperature} = E\{T_{EoD_{Time}}\} \quad (8)$$

4. SIMULATION AND EXPERIMENTAL RESULTS

For experimental validations a commercial lithium-ion 21700 cylindrical cell with nickel manganese cobalt oxide cathode and graphite node is utilised. The cell nominal capacity is 5.00Ah and its nominal voltage is 3.63V. The maximum and minimum allowable voltages are 4.2 and 2.5V respectively.

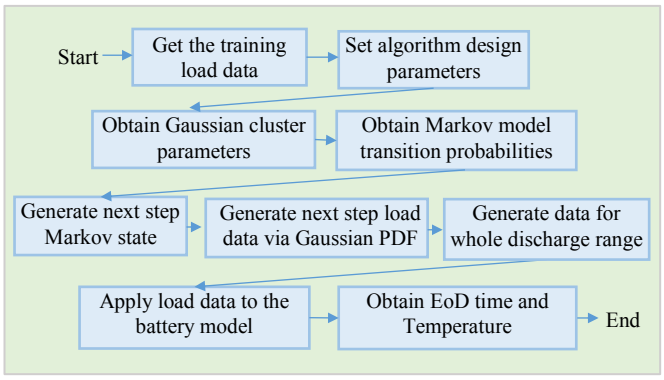

Fig. 3. The proposed algorithm steps

The V_{oc} as well as the parameters of the cell ECM are dependent to the battery SoC and estimated optimally via the experimental characterization procedure developed in (Chouchelamane, et al., 2015). The characterization test is run at 5, 10, 25 and 40 °C and the temperature averaged battery parameters are given in Fig. 4 for SoC intervals of 4%.

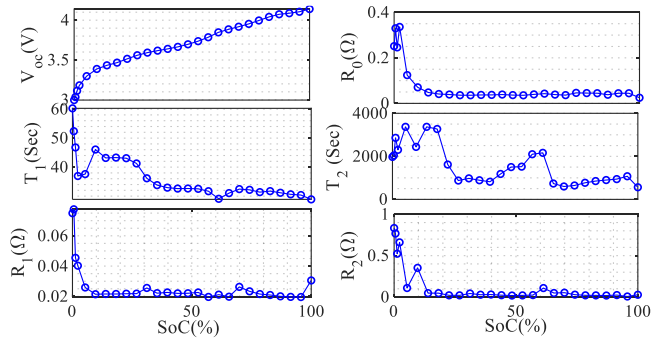

Fig.4. Temperature averaged battery model parameters

The parameters of battery thermal model are tuned based on the recommendations in the literature and the cooling mechanism in the thermal chamber. Thermal model parameters are given in Table I.

Table I. Battery thermal model parameters

Parameter	k_t [w m^{-1} K^{-1}]	Cell mass [kg]
Value	0.48 (Drake, et al., 2014)	0.068
Parameter	C_p [J kg^{-1} K^{-1}]	h [w m^{-2} K^{-1}]
Value	1050 (Loges, et al., 2016)	15

The root mean square error (RMSE) of the ECM and the thermal model is 40mV and 0.5 °C respectively. The cell temperature is measured at its surface via a thermocouple, while the modelled temperature is a volume averaged value, therefore the accuracy is believed to be acceptable for prediction purposes.

Notably, the load prediction mechanism is built based on a stochastic model and provides distinctive realizations in different runs. Here the number of realizations is set to 5 to characterise the future usage more confidently. Further analysis on the effect of the number of realizations on the accuracy of the results will be conducted in future studies.

Here, 4 cells are taken into account to minimise the cell to cell inconsistencies. In experiments the battery is preconditioned and fully charged (V_T = 4.2V, SoC=100%) at a desired temperature and then cycled by a loading profile. The experiments are ran with batteries inside a thermal chamber to mitigate the effect of ambient condition fluctuations. The experimental set up is shown in the fig.5.

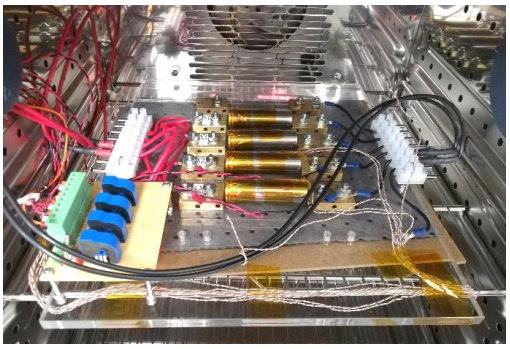

Fig.5. Experimental set up of the study

In order to investigate the capability of the method for EoD temperature prediction two loading scenarios are addressed. Both load profiles are obtained via time-velocity data and a vehicle model including a battery pack developed in (Taylor, et al., 2015). As a reference case the load prediction method is also compared with the moving average prediction of the load, which is called mean-based method here, considering similar length of historical data of 300 samples and update interval of 100 samples.

4.1. Case I: Artemis motorway load profile at 25°C

Artemis motorway load profile, Fig. 6, is one of the standard loading scenarios for automotive application studies.

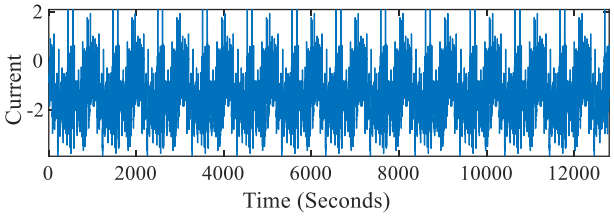

Fig. 6. Artemis motorway load profile

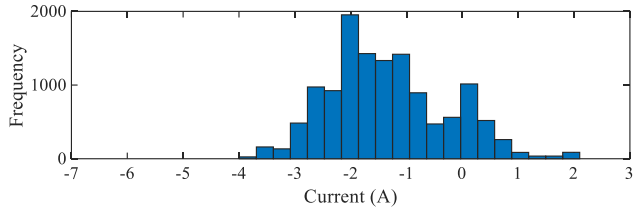

Fig.7. Histogram for Artemis motorway load profile

The histogram of the load data is given at Fig. 7 which shows a normal to intensive charge/discharge style.

The battery output voltage and its temperature is shown in the following figures 8 and 9 confirming the accuracy of the model. In this case the battery discharge process takes 12600 seconds. It is worth noting that thermal model also covers the cell cooling period (the time after 12600 seconds) which starts immediately after the discharge is terminated.

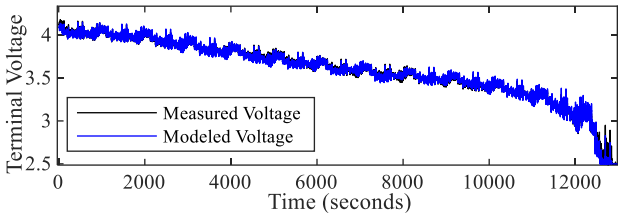

Fig.8. Battery terminal voltage under Artemis cycle

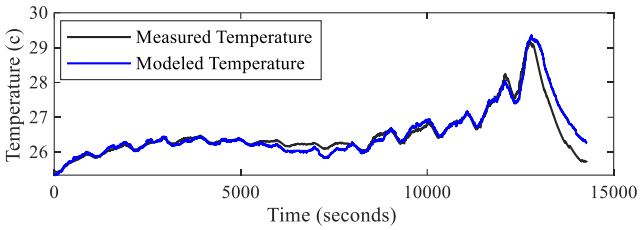

Fig.9. Measured and modeled temperature for Artemis cycle

The predicted EoD time and temperature is plotted at Fig. 10. As the figure shows the RMSE of temperature prediction is 0.84°C for Gaussian-Markov model-based prediction (GMPr) and 1.18 °C for mean-based prediction (MPr). This is due to increased accuracy of the predicted EoD time.

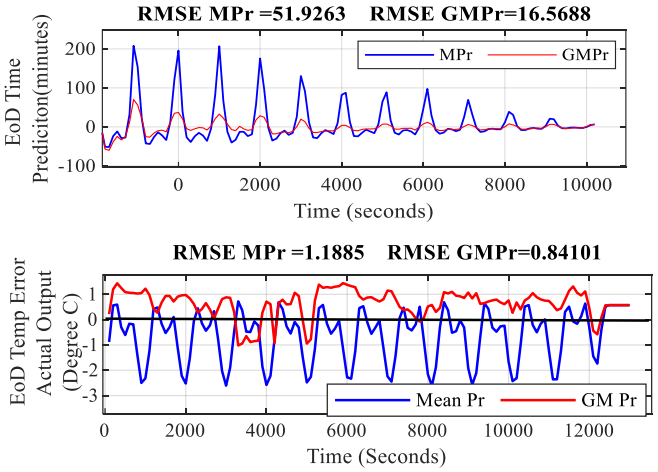

Fig.10. EoD time and temperature prediction for Artemis motorway cycle

To separate the modelling error from the load prediction algorithm error, Fig. 11 is developed which contains the prediction results assuming a perfect model availability. According to this figure the EoD temperature prediction error is 0.55 °C for GMPr method, i.e 65% of EoD temperature prediction error comes from load prediction algorithm and 34.2% is due to the battery modelling error.

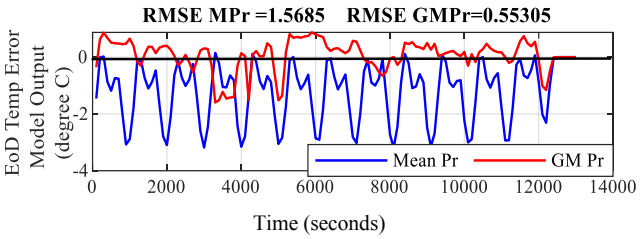

Fig.11. EoD temperature prediction for Artemis motorway cycle assuming a perfect model availability

4.2. Case II: Load profile of real driver at 10°C

This case study investigates a drive cycle recorded from a real driver at Coventry UK. The battery is cycled with this profile at 10 °C. The battery input current, output voltage and temperature is given in the Fig.12-15. The histogram of the input shows a rather intensive charge/discharge style and the battery voltage and temperature show the model accuracy.

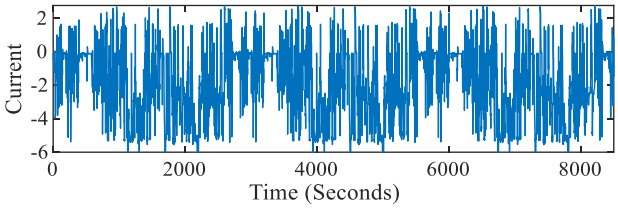

Fig.12. Battery input current for Coventry driving cycle

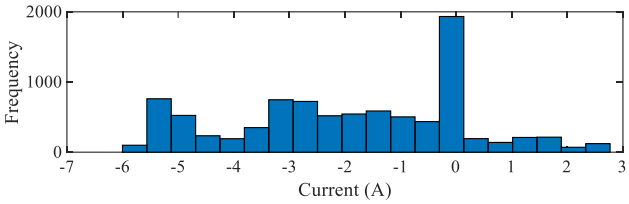

Fig.13. Histogram for Coventry driving cycle

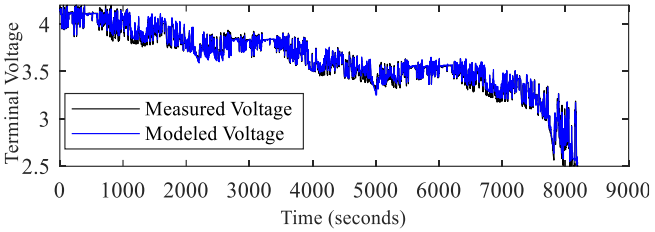

Fig.14. Battery terminal voltage under Coventry driving cycle

The EoD temperature prediction results are depicted in Fig. 16. In this case, the RMSE of temperature prediction is 2.26°C for

GMPr and 5.88 °C for MPr. Assuming a perfect model identification results are given in Fig. 17. For the GM Pr method 95.27 % of the error corresponds to load prediction algorithm while only 4.72% is due to the battery electrical-thermal modelling error.

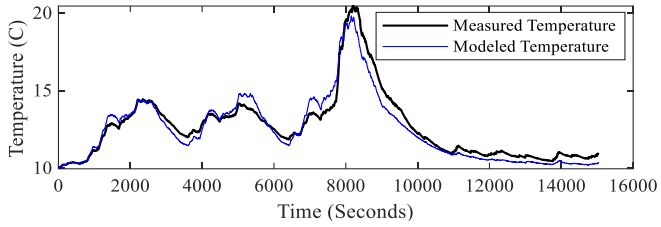

Fig.15. Measured and modeled temperature for Coventry driving cycle

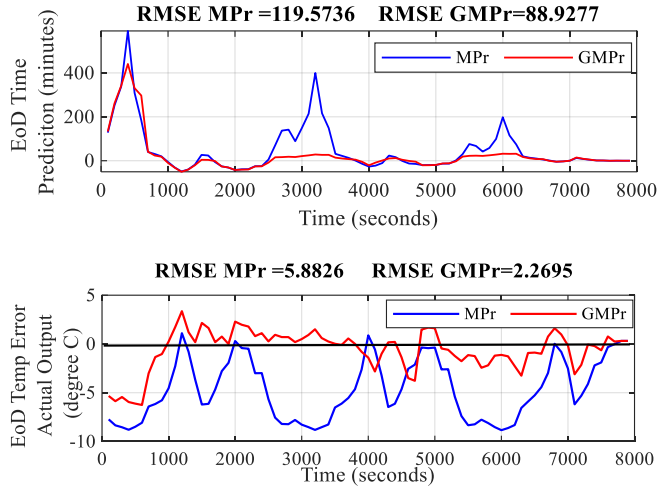

Fig.16. EoD time and temperature prediction for Coventry driving cycle

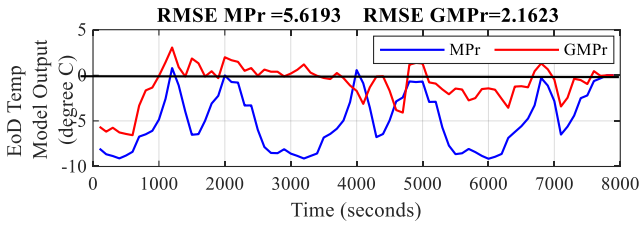

Fig.17. EoD temperature prediction for Coventry driving cycle assuming a perfect model availability

To understand the connection between the load style and the accuracy of the prediction method, example load profiles are applied to the battery with the same mean value but different peak limits; the results are reported in Table II. The table shows that the higher the discharge peak, the larger the prediction error. The reason is that higher peaks move the cluster centres away from average value and ultimately generate profiles with higher peaks that cause inaccurate determination of the EoD time and in turn the EoD temperature. For both scenarios the improvement over the mean-base prediction method is obvious. This is due to the capability of the proposed algorithm to deal with transient loads.

Table II: The effect of load style on the prediction accuracy

		EoD RMSE			
		Temperature (°C)		Time (minutes)	
		GMPr	MPr	GMPr	MPr
Loading Profile 1 Discharge Peak limit	-3 A	0.55	1.63	16.17	52.49
	-3.5 A	0.56	1.63	16.53	51.95
	-4 A	0.57	1.61	16.92	51.92
Loading Profile 2 Discharge Peak limit	-5 A	1.95	4.83	88.70	119.78
	-5.5 A	2.13	5.65	88.31	119.61
	-6 A	2.32	5.88	89.74	119.57

The time span of the whole simulation is 213 minutes for the profile 1 and 133 minutes for profile 2.

5. CONCLUSIONS

Battery thermal behaviour depends on its energy density as well as its charging C-rate. While both extremely high and low temperature can damage the battery, fast charging shifts the temperature balance of the cell towards higher temperature. Preheating the battery before a fast charging event is a solution for increasing the charge acceptability. Prediction of the battery temperature at the EoD and before fast charging can help the energy management for battery preconditioning. The algorithm in this paper facilitates an EoD temperature prediction validated by experiments. Further studies to improve the load prediction mechanism by selecting an optimal set of design parameters, including the training data interval as well as update interval is still required.

ACKNOWLEDGMENT

The research presented within this paper is supported by the Engineering and Physical Science Research Council (EPSRC - EP/I01585X/1) through the Engineering Doctoral Centre in High Value, Low Environmental Impact Manufacturing.

REFERENCES

Bernardi, D., Pawlikowski, E. & Newman, J., 1985. General energy balance for battery systems. *Journal of the Electrochemical Society,* 132(1), p. 5 – 12.

Brooks, S., Gelman, A., jones, G. L. & Meng, X.-L., 2011. *Handbook of Markov Chain Monte Carlo.* s.l.:CRC Press.

Cabañero, M. et al., 2019. Investigation of the temperature dependence of lithium plating onset conditions in commercial Li-ion batteries. *Energy,* Volume 171, pp. 1217-1228.

Chouchelamane, G. H. et al., 2015. A study on the impact of lithium-ion cell relaxation on electrochemical impedance spectroscopy. *Journal of Power Sources,* Volume 280, pp. 74-80.

Drake, S. et al., 2014 . Measurement of anisotropic thermophysical properties of cylindrical Li-ion cells. *Journal of Power Sources,* Volume 252, pp. 298-304.

Faraji Niri, M. et al., 2020. Remaining energy estimation for lithium-ion batteries via Gaussian mixture and Markov models for future load prediction. *Journal of Energy Storage,* Volume 8, p. 101271.

Faraji Niri, M., Marco, J., Dinh, T. & Yu, T., 2019. *Two Layer Markov Model for Prediction of Future Load and End of Discharge Time of Batteries.* Salerno, Italy, 23rd International Conference on Mechatronics Technology.

Hu , X., Li, S. & Peng, . H., 2012. A comparative study of equivalent circuit models for Li-ion batteries. *Journal of Power Sources,* Volume 198, pp. 359-367.

Jiang, B. & Fei, Y., 2015. *Traffic and vehicle speed prediction with neural network and hidden markov model in vehicular networks.* Seoul, South Korea, IV Intelligent Vehicles Symposium.

Ji, Y. & Wang, C., 2013. Heating strategies for Li-ion batteries operated from subzero temperatures. *Electrochimica Acta,* Volume 107, pp. 664-674.

Kim, Y., Siegel, J. B. & Stefanopoulou, A. G., 2013. *A Computationally Efficient Thermal Model of Cylindrical Battery Cells for the Estimation of Radially Distributed Temperatures.* Washington, DC, USA, American Control Conference, pp. 698-703.

Loges, A., Herberger, S., Seegert, P. & Wetzel, T., 2016. A study on specific heat capacities of Li-ion cell components and their influence on thermal management. *Journal of Power Sources,* Volume 336, pp. 341-350.

Lutsey, N., Searle, S., Chambliss, S. & Bandivadekar, A., 2015. *Assessment of leading electric vehicle promotion activities in United States cities,* Washington, DC: International Council on Clean Transportation.

Mussa, A. et al., 2017. Fast-charging to a partial state of charge in lithium-ion batteries: a comparative ageing study. *Journal of Energy Storage,* Volume 13, pp. 325-333.

Shah, K., McKee, C., Chalise, D. & Jain, A., 2016. Experimental and numerical investigation of core cooling of Li-ion cells using heat pipes. *Energy,* Volume 113, pp. 852-860.

Subramanian, . V. R., Diwakar, V. D. & Tapriyal, D., 2005. Efficient macromicro macromicro scale coupled modeling of batteries. *Journal of the Electrochemical,* 152(10), pp. 2002-2008.

Taylor, J. et al., 2015. Sizing tool for rapid optimisation of pack configuration at early-stage automotive product development. *World Electric Vehicle Journal,* 7(1), pp. 93-100.

Tech. rep., 2014. *2014 LEAF owner's manual,* s.l.: s.n.

Tomaszewska, A. et al., 2019. Lithium-ion battery fast charging: A review. *eTransportation,* Volume 1, p. 100011.

Trentadue, G. et al., 2018. Evaluation of fast charging efficiency under extreme temperatures. *Energies,* 11(8), pp. 1937-1950.

Wandt, J. et al., 2018. Quantitative and time-resolved detection of lithium plating on graphite anodes in lithium ion batteries. *Materials Today,* 21(3), pp. 231-240.

Wu, G., Zhu, C. & Chan, C., 2010. Comparison of the First Order and the Second Order Equivalent Circuit Model Applied in State of Charge Estimation for Battery Used in Electric Vehicles. *Journal of Asian Electric Vehicles,* 8(1), pp. 1357-1362.

Yang, X., Liu, T. & Wang, C., 2017. Innovative heating of large-size automotive Li-ion cells. *Journal of Power Sources,* Volume 342, pp. 598-604.

Yang, . X. & Wang , C., 2018. Understanding the trilemma of fast charging, energy density and cycle life of lithium-ion batteries. *Journal of Power Sources,* Volume 402, pp. 489-498.

Yang, X., Zhang, G., Ge, S. & Wang, C., 2018. Fast charging of lithium-ion batteries at all temperatures. *Proceedings of the National Academy of Sciences,* 115(28), pp. 7266-7271.

Zhang, L. & Peng, H., 2017. Comparative Research on RC Equivalent Circuit Models for Lithium-Ion Batteries of Electric Vehicles. *Applied Sciences,* 7(1002), pp. 1-16.

Zou, Y., Kong, Z., Liu, T. & Liu, D., 2016. A real-time Markov chain driver model for tracked vehicles and its validation: Its adaptability via stochastic dynamic programming. *IEEE Transactions on Vehicular Technology,* 66(5), pp. 3571-3582.